ELSEVIER

Electric Power Systems Research 54 (2000) 189–198

ELECTRIC POWER SYSTEMS RESEARCH

www.elsevier.com/locate/epsr

Distance protection in the presence of unified power flow controller

P.K. Dash *, A.K. Pradhan, G. Panda

Center for Intelligent Systems, Electrical Engineering Department, Regional Engineering College, Rourkela 769 008, India

Received 2 January 1999; received in revised form 19 April 1999; accepted 15 September 1999

Abstract

The presence of an important flexible AC transmission systems (FACTS) device like unified power flow controller (UPFC) can drastically affect the performance of a distance relay in a two-terminal system connected by a double-circuit transmission line. The control characteristics of the UPFC, its location on the transmission system and the fault resistance, especially the high ones make this problem more severe and complicated. The fault location with respect to the UPFC position also greatly influences the trip boundaries of the distance relay. The paper presents apparent impedance calculations for relaying of a double-circuit transmission system with varying UPFC parameters and location. The study reveals the adaptive nature of the protection scheme that necessitates the use of an artificial neural network (ANN) based procedure for the generation of trip boundaries during fault conditions.

Keywords: FACTS; UPFC; Distance protection; Trip boundary

1. Introduction

The rapid development of power electronics has made it possible to use high power electronic equipment for transmission systems. The concept of flexible AC transmission systems (FACTS) [1] envisages the use of solid state power converter technology for controlling the active and reactive power flow in the transmission line. The unified power flow controller (UPFC) [2] is the most versatile of the FACTS elements envisaged so far. The UPFC comprises of two voltage source converters connected by a capacitor charged to a DC voltage. One converter termed as the series voltage source converter injects a voltage of variable magnitude and phase angle which effectively modulates the reactance of the line, thereby altering the power flow of the line. The shunt converter, on the other hand, exchanges real power with the series branch drawn from the generating source as well as losses. If the power balance between the two converters is not maintained, the capacitor can not remain at a constant voltage.

Although the UPFC [3,4] improves the power flow in the transmission line, its presence imposes a number of problems including distance protection. The apparent impedance seen by a distance relay is influenced greatly [5] by the location and parameters of UPFC besides the fault resistance magnitude of the arc in case of a ground fault. If the impedance seen by a relay is lower or higher than the actual line impedance, the distance relay either overreaches or underreaches. Thus an adaptive relay setting of the distance protection is required to cope up with the problems of overreach or underreach.

Adaptive reach settings of the distance relays for faults involving high arc resistance have been researched [6–13] for sometime now. Methods for on-line corrections of the trip boundaries are presented in references [8–10]. This paper presents the apparent impedance calculation procedure along with detailed simulation results for distance relaying schemes in which the power transmission line has an UPFC. The variations of the UPFC parameters and the locations are found to influence the apparent impedance measurements and trip boundaries to a great extent.

* Corresponding author. Tel.: +91-661-576056; fax: +91-661-572926.

E-mail address: pkdash@rec.ori.nic.in (P.K. Dash)

0378-7796/00/$ - see front matter
PII: S0378-7796(99)00077-2

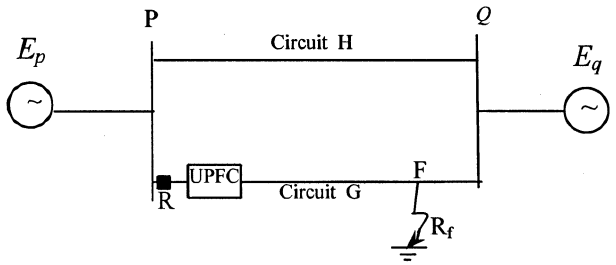

Fig. 1. Double circuit transmission system with UPFC.

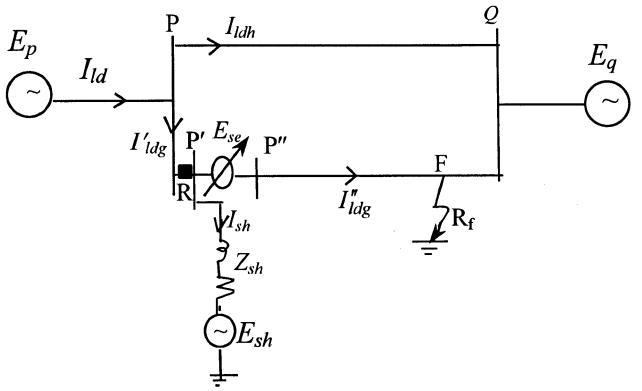

Fig. 3. UPFC located at relay point on circuit G.

2. Apparent impedance calculations

A double-circuit transmission line fed from both ends with varying UPFC location (either at the relay point or midpoint) subjected to a single line to ground fault as shown in Fig. 1 is considered. The UPFC is modeled by two voltage sources as shown in Fig. 2. The unified power flow controller is a recently proposed FACTS device that is capable of directing power flow through a desired route resulting in an increase in the usable capacity of the transmission lines. The UPFC consists of two AC/DC converters, one connected in series with the transmission line with a series transformer and the other connected in parallel with the line through a shunt transformer. The series and shunt converters are connected together through a DC capacitor, which also acts as an energy storage device. The series converter introduces a voltage source of variable magnitude and phase angle, while the shunt converter provides the real power balance between the series converter and the power system. The real power losses are also supplied by the shunt converter, which also maintains the DC bus voltage at a desired value. For apparent impedance calculations, the UPFC model equations hold good for the a-phase are

$$V_{ap'} = C_p V_{ap''} \tag{1}$$

$$\text{where } C_p = 1/(1+\gamma e^{j\theta}), \quad \gamma = \frac{|E_{se}|}{|V_{ap'}|} \tag{2}$$

The magnitude of E_{se} can be controlled by varying the dc voltage and firing angle of the series voltage source converter and θ varies from 0 to 2π radians. The shunt current is obtained as

$$I_{ash} = (V_{ap'} - E_{sh})/Z_{sh}$$

$$E_{sh} = V_{ap'}/C_{sh} \tag{3}$$

Where E_{sh} = shunt converter voltage, C_{sh} = voltage ratio ($V_{ap'}/E_{sh}$) and Z_{sh} is its impedance. Assume E_{ap} as the equivalent voltage source of the a-phase at the terminal P. Let the relation between bus voltage at P and E_{ap} be

$$V_{ap} = h e^{-j\delta} E_{ap} \tag{4}$$

Where h is the amplitude ratio (V_{ap}/E_{ap}) and δ is the angle between the source voltage and bus voltage at P. The apparent impedance as seen by the phase to ground relay for both line to ground and double line to ground faults are derived in the following sections.

2.1. Line to ground fault

2.1.1. UPFC at the relaying point

A two terminal model with equivalent generating sources, source impedances and a double circuit line is shown in Fig. 3. The UPFC is placed on circuit G at

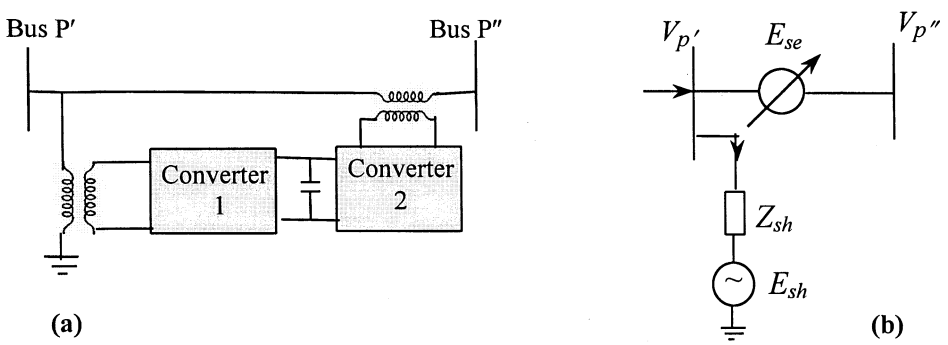

Fig. 2. (a) Basic circuit arrangement of UPFC; (b) its equivalent voltage representation.

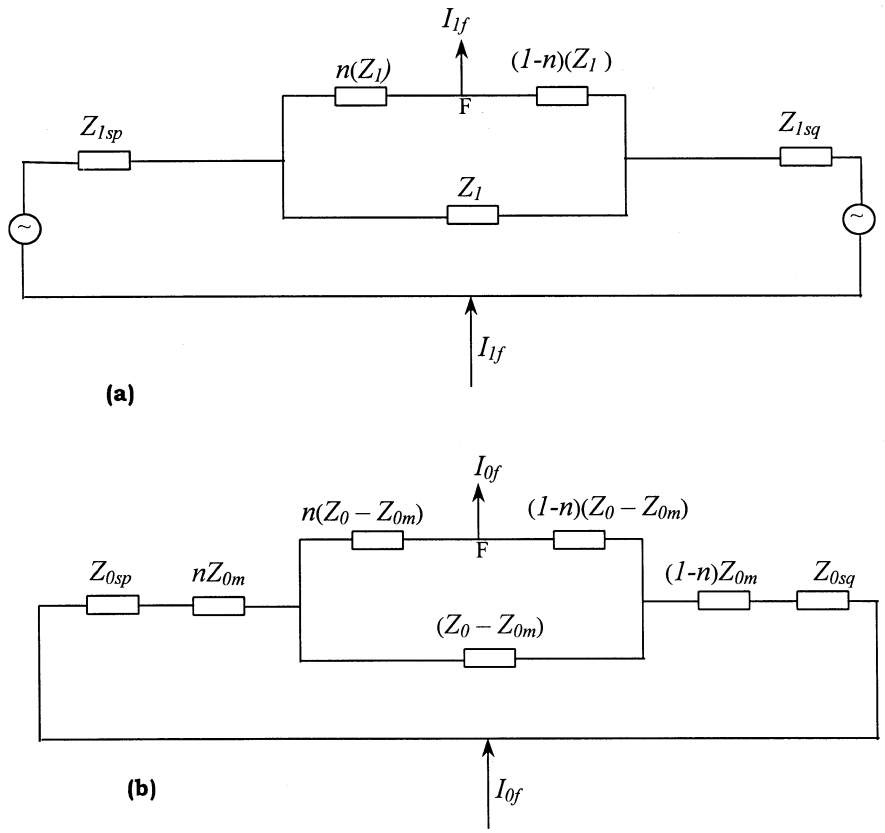

Fig. 4. (a) Positive sequence network; (b) zero-sequence network of the faulted power system.

the relay point R. A single-line-to ground fault is considered on the circuit at the point F as shown in Fig. 3.

The prefault a-phase currents I'_{aldg} and I''_{aldg} are given by,

$$I''_{aldg} = I'_{aldg} - I_{ash}$$

$$I'_{aldg} = I_{ash} + I_{aldh} + \gamma\, e^{j\theta} V_{ap}/Z_1 \quad (5)$$

Again

$$I_{ald} = I'_{aldg} + I_{aldh} = (E_{ap} - V_{ap})/Z_{1sp}$$

$$I''_{aldg} = (V_{ap''} - V_{afd})/Z_{1pf} \quad (6)$$

Where Z_1 is the positive sequence impedance of each circuit, V_{afd} is the a-phase voltage at the fault point, Z_{1pf} is the positive sequence impedance of the line between the bus P and F. From the above we get

$$V_{ap} = C_{vp} I_{of} \quad (7)$$

where $C_{vp} = -(3R_f + Z_\Sigma)$
$/((1/he^{-j\delta} - 1)(Z_{1pf}/2Z_{1sp})$
$+ ({}^1/_{C_p} - 1)(Z_{1pf}/2Z_1)$
$+ ({}^1/_{C_{sh}} - 1)(Z_{1pf}/2Z_{sh}) - 1/C_p)$ (8)

and $Z_\Sigma = Z'_0 + Z'_1 + Z'_2$ (refer Eqs. (11) and (12))

I_{of} being zero sequence component of fault current.

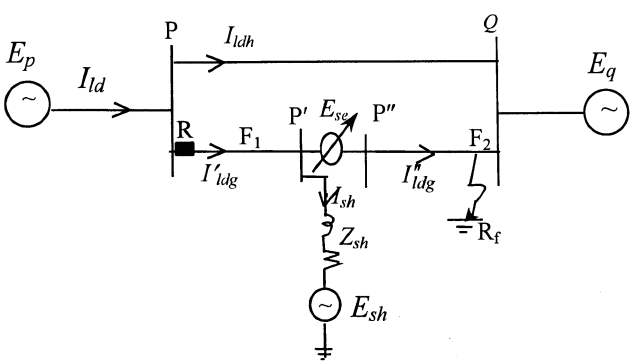

Fig. 5. UPFC placed at the midpoint of circuit G.

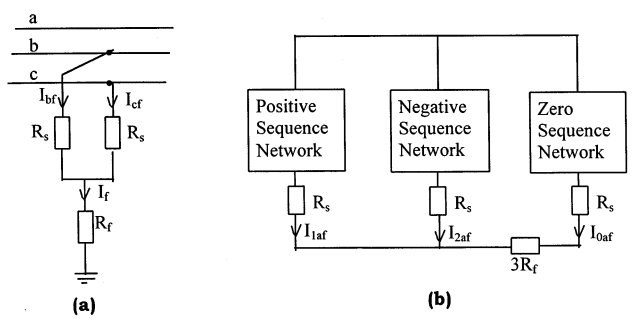

Fig. 6. (a) Double line to ground fault; (b) its sequence network.

Table 1
UPFC at relay point $R_f = 5\ \Omega$ (LG fault)

γ	$\theta = 0°$		$\theta = 90°$		$\theta = 270°$	
	X_a (Ω)	R_a (Ω)	X_a (Ω)	R_a (Ω)	X_a (Ω)	R_a (Ω)
0.0	50.5908	36.0607	50.5908	36.0607	50.5908	36.0607
0.1	31.0773	17.7354	42.1176	33.7448	53.8599	30.6256
0.2	22.6156	12.0594	39.0785	37.8262	57.2116	25.3201
0.3	18.0566	9.3764	34.0785	39.3516	59.6673	19.4128
0.4	15.2432	7.8142	30.7696	39.9905	60.9176	13.1384
0.5	13.3456	6.7857	26.9737	40.0378	60.8838	6.8812

Table 2
UPFC at midpoint $R_f = 5\ \Omega$ (LG fault)

γ	$\theta = 0°$		$\theta = 90°$		$\theta = 270°$	
	X_a (Ω)	R_a (Ω)	X_a (Ω)	R_a (Ω)	X_a (Ω)	R_a (Ω)
0.0	50.5908	36.0607	50.5908	36.0607	50.5908	36.0607
0.1	52.1967	28.9979	46.9559	35.4266	55.7043	34.7019
0.2	51.5853	24.8496	42.7129	34.7799	60.4855	32.0572
0.3	50.5019	22.0761	39.5357	33.3974	64.5156	28.1156
0.4	49.3515	20.0572	37.1140	31.7706	67.3434	23.2350
0.5	48.2499	18.5025	35.3035	30.1212	68.7508	17.9531

Table 3
UPFC at relay point $R_f = 5\ \Omega$, $R_s = 0.1\ \Omega$ (L-L-G fault)

γ	$\theta = 0°$		$\theta = 90°$		$\theta = 270°$	
	X_b (Ω)	R_b (Ω)	X_b (Ω)	R_b (Ω)	X_b (Ω)	R_b (Ω)
0.0	40.6127	21.7014	40.6127	21.7014	40.6127	21.7014
0.1	32.8990	23.6164	36.5635	24.9269	42.9384	18.9357
0.2	27.2722	23.9376	34.1586	26.3771	45.0541	15.4016
0.3	23.2214	23.4735	31.3410	27.6506	46.5585	11.3491
0.4	20.2987	22.6509	28.5510	28.5521	47.2697	7.0062
0.5	18.1669	21.6858	25.8578	29.1142	47.1286	2.6415

Table 4
UPFC at midpoint $R_f = 5\ \Omega$, $R_s = 0.1\ \Omega$ (L-L-G fault)

γ	$\theta = 0°$		$\theta = 90°$		$\theta = 270°$	
	X_b (Ω)	R_b (Ω)	X_b (Ω)	R_b (Ω)	X_b (Ω)	R_b (Ω)
0.0	40.6127	21.7014	40.6127	21.7014	40.6127	21.7014
0.1	41.9593	19.1140	38.9589	21.3554	43.2515	21.4372
0.2	42.0219	17.2731	36.9938	20.7447	45.8777	20.4694
0.3	41.6575	15.8829	35.6343	19.9915	48.2795	18.7665
0.4	41.1450	14.7832	34.6394	19.2550	50.1911	16.4563
0.5	40.5918	13.8837	33.8902	18.6084	51.4419	13.7758

Further I''_{aldg} and I_{ash} are rewritten as

$$I''_{aldg} = C_{ldd} I_{of}, \quad I_{ash} = C_{lsh} I_{of} \tag{9}$$

Where $C_{ldd} = \left(\dfrac{C_{vp}}{C_p} - (3R_f + Z_\Sigma)\right) \Big/ Z_{1pf}$ and

$$C_{lsh} = C_{vp}(1 - 1/C_{sh})/Z_{sh} \tag{10}$$

The magnitudes of Z'_0, Z'_1 ($Z'_2 = Z'_1$) are obtained from the equivalent sequence diagrams as shown in Fig. 4.

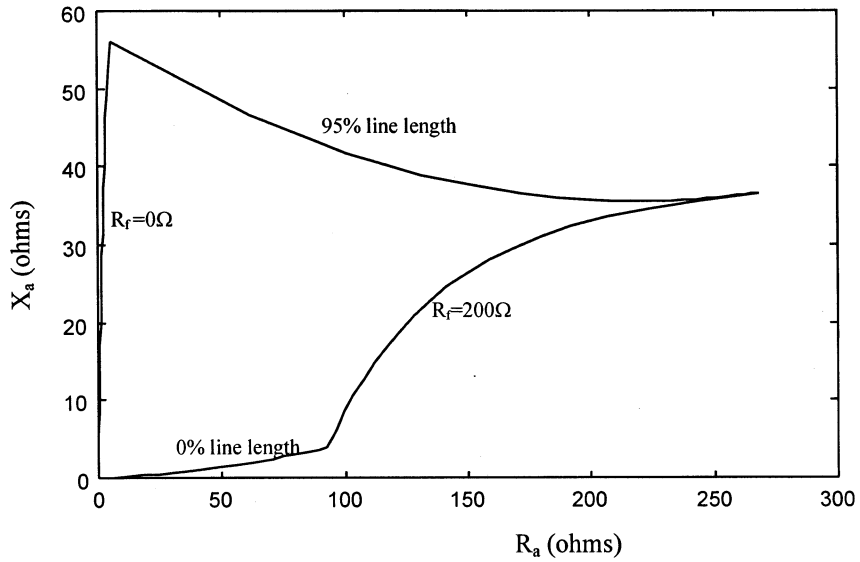

Fig. 7. Trip characteristic without UPFC for LG fault.

$$Z_1' = \frac{n(1-n)Z_1}{2} + \frac{\left(Z_{1sp} + \frac{nZ_1}{2}\right)\left(Z_{1sq} + \frac{(1-n)Z_1}{2}\right)}{Z_{1sp} + Z_{1sq} + \frac{Z_1}{2}} \tag{11}$$

$$Z_0' = \frac{\left(Z_{osp} + n\frac{(Z_{0m} + Z_0)}{2}\right)\left(Z_{osq} + \frac{(1-n)(Z_{om} + Z_0)}{2}\right)}{Z_{osp} + Z_{0sq} + \frac{Z_{om} + Z_0}{2}} + n(1-n)\frac{(Z_0 - Z_{om})}{2} \tag{12}$$

Where Z_{1sp}, Z_{1sq}, Z_{osp}, Z_{0sq} = positive and zero sequence impedances of the sources at the terminals P and Q, respectively. Z_{om} = zero sequence mutual impedance between circuit G and circuit H. n = per unit distance of the fault point F from the relaying point R.

The relay current (I_{aR}) and voltage (V_{aR}) of a-phase are obtained as

$$I_{aR} = I''_{aldg} + I_{ash} + I_{ap''f} + K_0 I_{op''f} \tag{13}$$

Where the a-phase fault current at P″ (UPFC injection bus) is

$$I_{ap''f} = I_{1ap''f} + I_{2ap''f} + I_{oap''f}$$

The suffixes 1, 2, and 0 pertain to the positive, negative and zero sequences, respectively, and the zero sequence compensation factor $K_0 = (Z_0 - Z_1)/Z_1$.

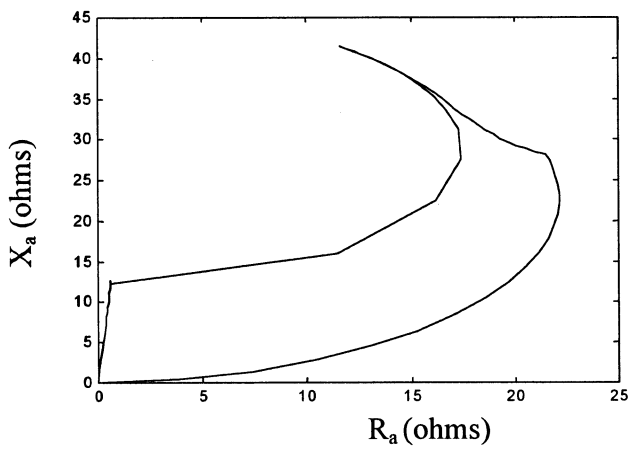

Fig. 8. Trip characteristics for UPFC at relay point, $\Upsilon = 0.5$; $\theta = 0°$ (LG fault).

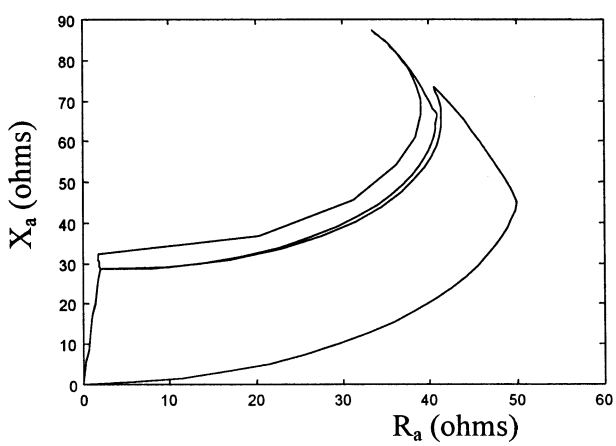

Fig. 9. Trip characteristics for UPFC at midpoint, $\Upsilon = 0.5$; $\theta = 0°$ (LG fault).

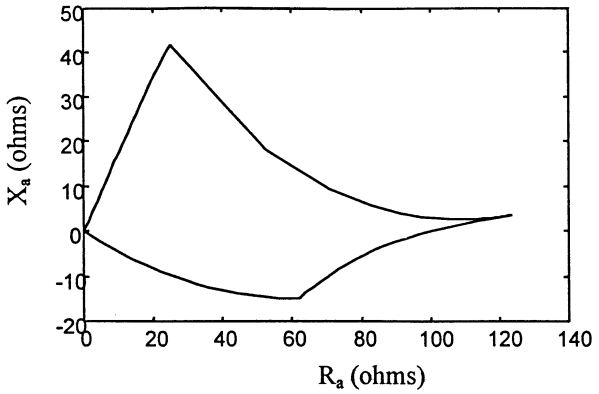

Fig. 10. Trip characteristics for UPFC at relay point, $\Upsilon = 0.5$; $\theta = 90°$ (LG fault).

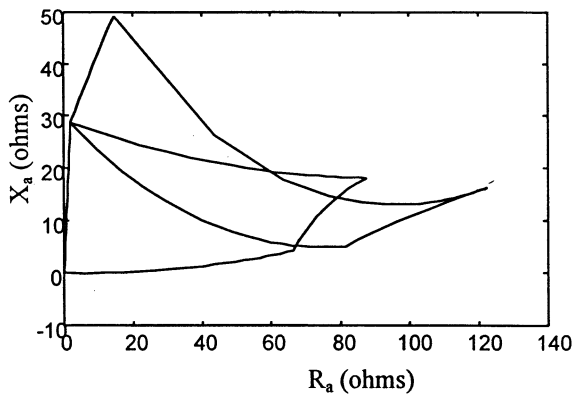

Fig. 11. Trip characteristics for UPFC at midpoint, $\Upsilon = 0.5$; $\theta = 90°$ (LG fault).

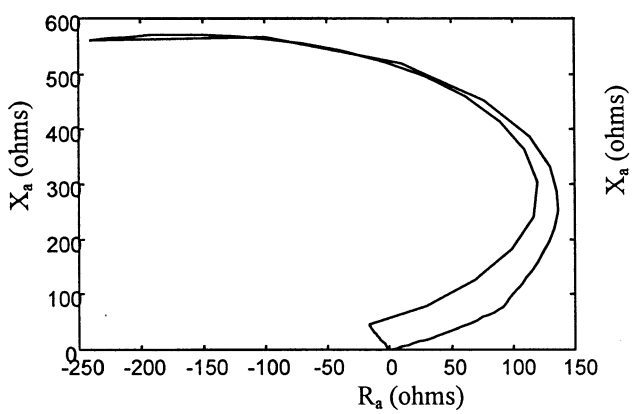

Fig. 12. Trip characteristics for UPFC at relay point, $\Upsilon = 0.5$, $\theta = 270°$ (LG fault).

$$V_{aR} = C_p(3R_fI_{of} + I_{1ap''f}Z_{1pf} + I_{2ap''f}Z_{2pf} + I_{oap''f}Z_{opf} + I_{oh}nZ_{om} + I''_{ld}Z_{1pf}) \quad (14)$$

Substituting Z_{1pf} by nZ_1, the apparent impedance seenby a-phase to ground relay is obtained as

$$Z_a = \frac{V_{aR}}{I_{aR}} = C_p(nZ_1 + \Delta Z) \quad (15)$$

where

$$\Delta Z = \frac{3R_f + C_m nZ_{om} - nZ_1C_{lsh}}{C_{ldd} + C_{lsh} + 2C_1 + C_0(1 + K_0)} \quad (16)$$

$$C_m = \frac{nZ_{osq} - (1-n)Z_{osp}}{2Z_{osp} + Z_0 + Z_{om} + 2Z_{osq}} \quad (17)$$

$$C_0 = \frac{(2-n)Z_{osq} + (1-n)(Z_0 + Z_{om} + Z_{osp})}{2Z_{osp} + Z_0 + Z_{om} + 2Z_{osq}} \quad (18)$$

$$C_1 = \frac{(2-n)Z_{1sq} + (1-n)(Z_1 + Z_{1sp})}{2Z_{1sp} + Z_1 + 2Z_{1sq}} \quad (19)$$

From Eq. (15) it can be observed that if the UPFC is placed at the relaying point on one of the circuits of the double circuit transmission line, the apparent impedance seen by the relay for a single-line-to-ground fault is influenced by the factor C_p of the UPFC. Also the incremental impedance ΔZ is influenced by the resistance R_f in the fault path, zero sequence mutual impedance, UPFC shunt branch current, fault location and prefault system condition.

2.1.2. UPFC at the midpoint of one circuit

In the above configuration (Fig. 5) the fault can occur at F_1 on one of the line section that does not include the UPFC, where as the fault occurring at F_2 includes the UPFC and thus influences the apparent impedance seen by the relay. If the fault occurs at F_2, the apparent impedance Z_a seen by a-phase to ground relay is given by

$$Z_a = \frac{Z_1}{2} + C_p(n - {}^1/_2)Z_1 + \Delta Z' \quad (20)$$

where

$$\Delta Z' = \frac{3R_fC_p + C_m\left(C_p(n - {}^1/_2)Z_{om} + \frac{Z_{om}}{2}\right) - C_{lsh}C_p(n - {}^1/_2)Z_1}{C_{ldd} + C_{lsh} + 2C_1 + C_0(1 + K_0)} \quad (21)$$

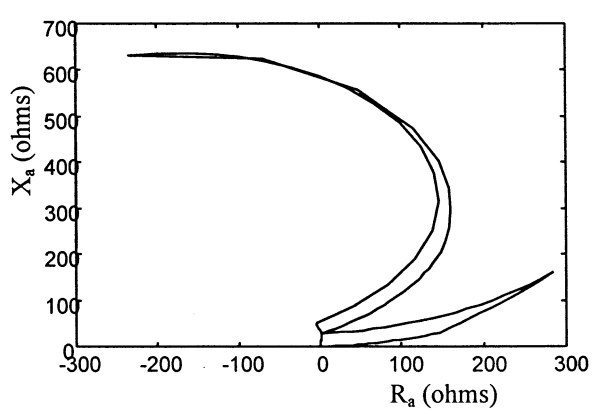

Fig. 13. Trip characteristics for UPFC at midpoint, $\Upsilon = 0.5$; $\theta = 270°$ (LG fault).

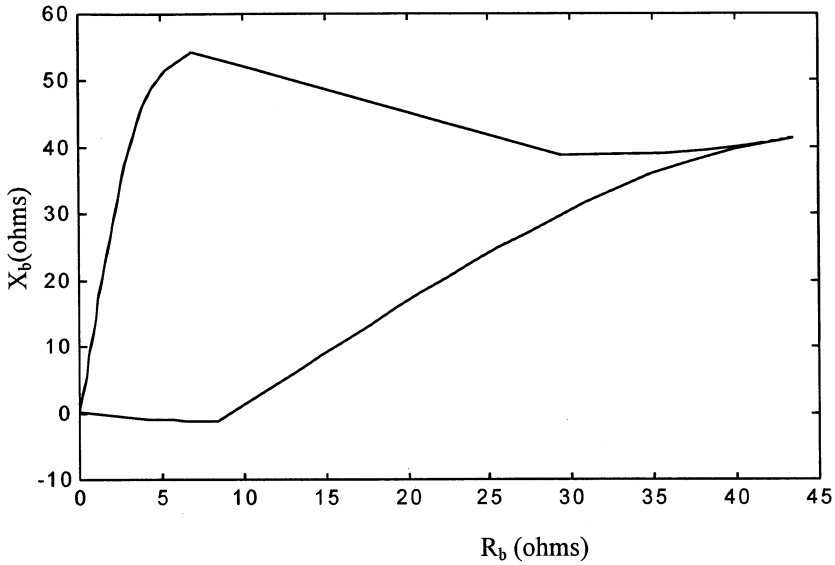

Fig. 14. Trip characteristics without UPFC for LLG fault.

Similarly for a fault at F_1 the value of Z_a is

$$Z_a = nZ_1 + \frac{3R_f + C_m nZ_{0m}}{C_{ldd} + C_{lsh} + 2C_1 + C_0(1 + K_0)} \quad (22)$$

2.2. Double line to groundfault

In furthering the study on the effect of UPFC on apparent impedance, a double-line to ground fault (b-c-g) is initiated and the impedance seen by one of the ground elements (b phase to ground) is calculated. In the fault path besides R_f another fault resistance R_s is considered between phase to phase as shown in Fig. 6(a). The sequence network (Fig. 6(b)) for such a case is used to derive the seen impedance.

$$I_{0af} = -\left[\frac{Z'_2 + R_s}{(Z'_2 + R_s) + (Z'_0 + R_s + 3R_f)}\right] I_{1af}$$

$$I_{2af} = -\left[\frac{Z'_0 + R_s + 3R_f}{(Z'_2 + R_s) + (Z'_0 + R_s + 3R_f)}\right] I_{1af} \quad (23)$$

Let $I_{1af} = CC_1 I_{0af}$ and $I_{2af} = CC_2 I_{0af}$

Hence $I_{1bf} = \alpha^2 CC_1 I_{0af}$, $I_{2bf} = \alpha CC_2 I_{0af}$, $I_{1cf} = \alpha CC_1 I_{0af}$, $I_{2cf} = \alpha^2 CC_2 I_{0af}$ where

$$CC_1 = -\frac{(Z'_2 + Z'_0 + 2R_s + 3R_f)}{(Z'_2 + R_s)}$$

$$CC_2 = -\frac{(Z'_0 + R_s + 3R_f)}{(Z'_2 + R_s)(Z'_0 + R_s + 3R_f)} \cdot CC_1 \quad (24)$$

and α is the 120° shift operator.

$$3I_{0f} = I_{bf} + I_{cf} = (2 - CC_1 + CC_2) I_{0af}$$

$$V_{afd} = \left((Z'_1 + R_s) + \frac{(Z'_2 + R_s)(Z'_0 + R_s + 3R_f)}{(Z'_2 + R_s)(Z'_0 + R_s + 3R_f)}\right) CC_1 I_{0af}$$

$$= C_{afd} I_{0af} \quad (25)$$

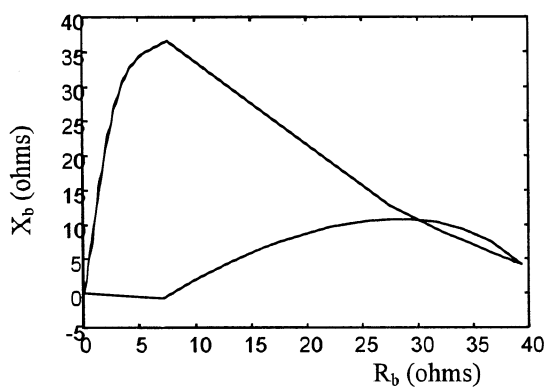

Fig. 15. Trip characteristics for UPFC at relay point, $\Upsilon = 0.5$; $\theta = 0°$ (LLG fault).

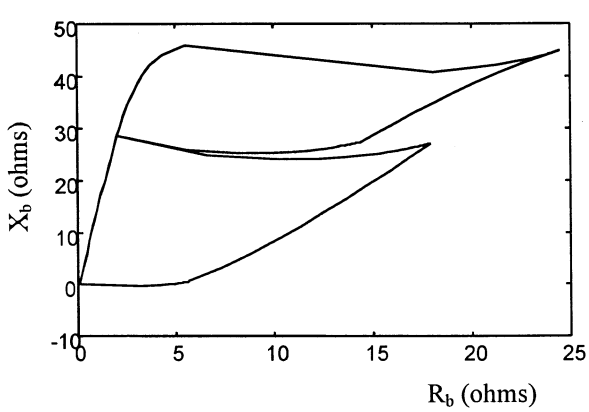

Fig. 16. Trip characteristics for UPFC at midpoint, $\Upsilon = 0.5$; $\theta = 0°$ (LLG fault).

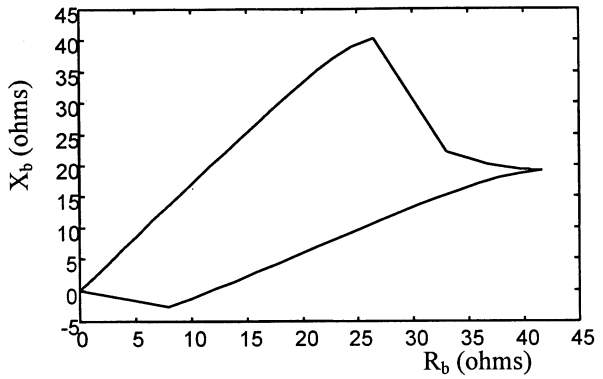

Fig. 17. Trip characteristics for UPFC at relay point, $\Upsilon = 0.5$; $\theta = 90°$ (LLG fault).

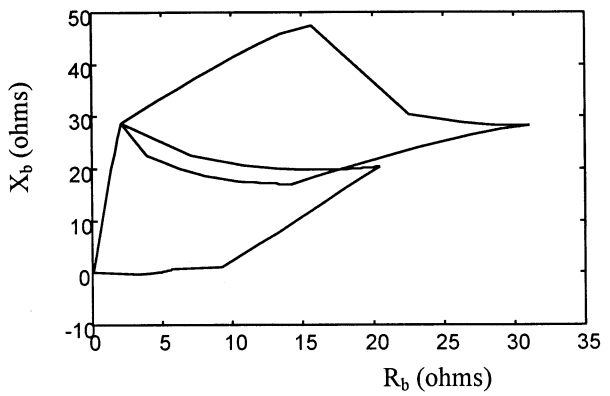

Fig. 18. Trip characteristics for UPFC at midpoint, $\Upsilon = 0.5$; $\theta = 90°$ (LLG fault).

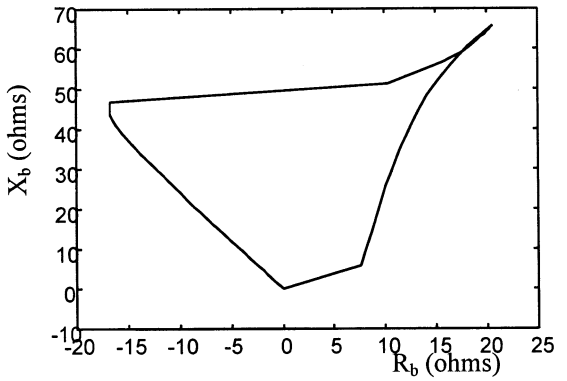

Fig. 19. Trip characteristics for UPFC at relay point, $\Upsilon = 0.5$; $\theta = 270°$ (LLG fault).

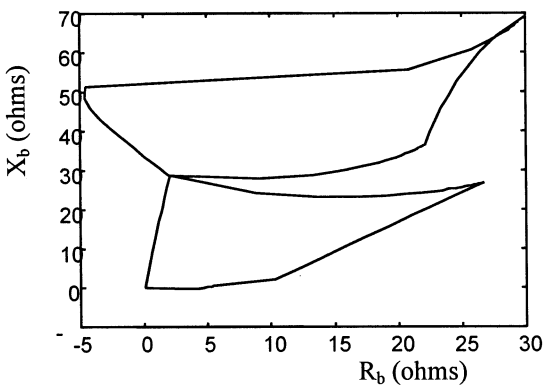

Fig. 20. Trip characteristics for UPFC at midpoint, $\Upsilon = 0.5$; $\theta = 270°$ (LLG fault).

where

$$C_{afd} = \left((Z_1' + R_s) + \frac{(Z_2' + R_s)(Z_0' + R_s + 3R_f)}{(Z_2' + R_s)(Z_0' + R_s + 3R_f)} \right) CC_1$$

2.2.1. UPFC at relay location

Using Eqs. (1)–(6) and Eqs. (23)–(25) we can deduce the apparent impedance seen by the b phase to ground element in the case of b-c-g fault as

$$Z_b = C_p n Z_1 + \frac{C_p\{R_f(2-(CC_1-CC_2)) + C_m n Z_{0m} - \alpha C_{lsh} n Z_1 + R_s(\alpha CC_2 + \alpha^2 CC_1 + 1)\}}{C_{1dd} + \alpha C_{lsh} + \alpha CC_2 C_2 + \alpha^2 CC_1 C_1 + C_0(1+K_0)} \quad (26)$$

2.2.2. UPFC at midpoint of one circuit

For faults beyond UPFC (b-c-g type) at F_2 in Fig. 5

$$Z_b = \frac{Z_1}{2} + C_p\left(n - \frac{1}{2}\right) Z_1 + \Delta Z' \left[R_f C_p (2 - (CC_1 + CC_2)) + C_m \left(C_p \left(n - \frac{1}{2} \right) Z_{0m} + \frac{Z_{0m}}{2} \right) \right] \quad (27)$$

where $\Delta Z'$

$$= \frac{R_s C_p(\alpha CC_2 + \alpha^2 CC_1 + 1) + C_{lsh} C_p \left(n - \frac{1}{2} \right) Z_1 \Big]}{C_{1dd} + C_{lsh} + \alpha CC_2 C_2 + \alpha^2 CC_1 C_1 + C_0(1+K_0)} \quad (28)$$

For faults within UPFC, F_1 in Fig. 5

$$Z_b = nZ_1 + \frac{R_f(2-(CC_1+CC_2)) + R_s(\alpha CC_2 + \alpha^2 CC_1 + 1) + C_m n Z_{0m}}{C_{1dd} + C_{lsh} + \alpha CC_2 \cdot C_2 + \alpha^2 CC_1 \cdot C_1 + C_0(1+K_0)} \quad (29)$$

3. Simulation results

The 200 km, 400 kV double-circuit transmission line considered for computer simulation has the following data:

Positive sequence impedance of line = $0.0201 + j$ 0.2868 Ω/km
Zero sequence impedance of line = $0.1064 + j$ 0.8670 Ω/km
Zero sequence mutual impedance of line = $0.1718 + j$ 0.6930 Ω/km
Parameters for sources at P and Q are
$Z_{1sp} = 1.7431 + j$ 19.424 Ω, $Z_{1sq} = 0.8716 + j$ 9.7120 Ω
$Z_{0sp} = 2.6147 + j$ 4.886 Ω, $Z_{0sq} = 1.3074 + j$ 2.4430 Ω
Amplitude ratio between source voltages at P and Q = 0.95
Load angle between sources = 20°

The value of γ of the unified power flow controller is varied between 0 and 0.5, while that of θ is varied between 0 and 360°. The shunt voltage source converteris represented by an equivalent voltage source E_{sh} and impedance $Z_{sh} = 0.3 + j$ 5.0 Ω, respectively. The magnitude of the shunt converter voltage source E_{sh} is computed from the power balance equation:

$$Re(V_{ap'} I^*_{ash}) = Re(\gamma V_{ap'} e^{j\theta} I^*_{aldg}) \quad (30)$$

A single-line-to ground fault is assumed to occur at the point F shown in Fig. 1 at a distance of 95% of the length of the circuit G. Table 1 shows the apparent resistance R_a and reactance X_a seen by the relay; the real and imaginary parts of Z_a, respectively, for values of γ varying from 0 to 0.5 and θ at discrete angles of 0, 90 and 270°. The fault resistance R_f is assumed to be 5 Ω. The location of the UPFC is now changed to the midpoint of the transmission line of the circuit G. Table 2 exhibits the variations in R_a and X_a for different values of γ and θ.

From the above results it can be seen that for the UPFC placed near the relaying point (Table 1) and $\theta = 0°$, the resistance and reactance seen by the relay decrease in magnitude with the increase of γ from 0 to 0.5. However, at $\theta = 90°$, as γ increases from 0 to 0.5, the resistance R_a varies from its initial value of 36.06 to 40.03 Ω, whereas the reactance X_a decreases drastically from 50.59 to 26.97 Ω. At an angle of $\theta = 270°$, the resistance R_a decreases drastically from 36.06 to 6.88 Ω, whereas the reactance X_a increases from 50.59 to 60.88 Ω.

From the results in Table 2 the seen reactance X_a with UPFC at midpoint of circuit G for $\theta = 0°$ and γ increased from 0.0 to 0.5 shows complex variation whereas the resistance decreases from 36.06 to 18.50 Ω. The apparent reactance for $\theta = 90°$ decreases from 50.59 to 35.03 Ω, however, the resistance value decreases as γ increases from 0.0 to 0.5. At $\theta = 270°$ the resistance decreases drastically and the reactance shows a complex variation. These variations clearly demonstrate that the presence of the UPFC introduces a capacitive or inductive reactance to the line depending on its parameters γ and θ and the location.

For the same system condition as in Table 1, with UPFC at relay point and $R_s = 0.1$ Ω; and $R_f = 5$ Ω double line to ground (b-c-g) fault is initiated at the reach point (95%). The impedance seen by the b phase to earth element is tabulated for different values of γ and θ (Table 3). With increasing γ from 0.0 to 0.5 and $\theta = 0°$ the reactance seen by b phase to ground element decreases from 40.61 to 18.16 Ω and the resistance values show a complex variation. At $\theta = 90°$ the X_b decreases significantly from 40.61 to 25.85 Ω and on the other hand R_b increases from 21.70 to 29.11 Ω. However at $\theta = 270° X_b$ shows an increasing trend and R_b decreases drastically from 21.70 to 2.64 Ω.

The calculation of seen impedance for double line to ground fault with UPFC at midpoint of circuit G also shows an analogous behavior. Table 4 enumerates some of the results for such a case. With θ set at 0° the reactance shows a complex variation and the reactance decreases from 21.70 to 13.88 Ω. For $\theta = 90°$ both X_b and R_b decrease with γ increasing from 0.0 to 0.5. The X_b values show upward trend whereas the R_b values decrease from 21.70 to 13.77 Ω. Similar to earlier observation the UPFC influences the apparent impedance seen by one of the ground elements significantly even in the case of double line to ground fault, as expected.

4. Trip characteristics

4.1. Line to groundfault

The system operating conditions described by h, δ, Z_{sp}, Z_{sq} are kept constant and the fault location in km on one of the circuit and fault resistance R_f (from 0 to 200 Ω) are varied to provide the trip characteristics of the parallel transmission systems with and without UPFC. Fig. 7 depicts the trip characteristic without the presence of UPFC for line to ground fault. However, if the UPFC is located at the midpoint, the trip characteristic exhibits two different trip boundaries, the upper one for faults between the midpoint and to 95% of the line length (R_f varying from 0 to 200 Ω). The lower characteristic is due to the fault location lying between the relaying point to the midpoint where the UPFC is located. Figs. 8–13 represent the trip boundaries for line to ground fault with the presence of UPFC either at relaying point or midpoint of circuit G for θ values of 0, 90 and 270° keeping γ unchanged ($\gamma = 0.5$). In Fig. 8 it is observed that for $\theta = 0°$ and UPFC at relaying point the trip area is reduced significantly as both R_a and X_a values are decreased. With same system conditions with the UPFC at midpoint of circuit G ($\theta = 0°$), the upper characteristic boundary shows complex variation in both X_a and R_a (Fig. 9). Though the range of X_a is increased in this case that of R_a is decreased signifi-

cantly from 250 to 50 Ω approximately. Figs. 10 and 11 demonstrate for $\theta = 90°$ case with UPFC at relaying point and midpoint respectively and in both the locations of UPFC the upper boundary declines with higher R_f. At $\theta = 270°$ the area is significantly increased for both UPFC positions as demonstrated in Figs. 12 and 13. The value of X_a swings up to 600 Ω high as compared to 60 Ω in Fig. 7. Noticeably the value of R_a becomes negative and again as high as − 250 Ω. These figures clearly justify the influence of UPFC parameters and position on the trip boundary set for line to groundfault.

4.2. Double line to groundfault

With $R_s = 0.1$ Ω, R_f varying from 0 to 200 Ω, keeping system operating condition remaining same as earlier, the influence of UPFC to the seen impedance of b phase to ground element for double line to ground fault (b-c-g) is examined in this section. Fig. 14 depicts the trip boundary for such a fault without the presence of UPFC. At $\theta = 0°$, for UPFC at relaying point the trip area is reduced significantly (Fig. 15) whereas for UPFC at midpoint the trip boundary is not affected significantly (Fig. 16). Similar effects are observed for the case of $\theta = 90°$ as shown in Figs. 17 and 18. At $\theta = 270°$ the upper boundary is at higher level for both positions of UPFC (Figs. 19 and 20). These boundaries in Figs. 15–20 show the influence of UPFC parameters and position on the trip characteristics of a distance relay for double line to groundfault.

5. Discussions

From the results described in the preceding section, it can be observed that the trip boundaries of the relay are influenced significantly by the presence of the UPFC and its exact location. The parameters γ and θ of UPFC make the total impedance seen by the relay small or large making it either an equivalent capacitance or inductance. The low or high magnitude of the earth fault resistance R_f alters the trip area significantly. Thus to provide a suitable trip boundary for faults on a double-circuit line, the boundary needs to be manipulated adaptively with γ and θ of the UPFC on the time. This adaptation can be carried out using a neural network whose weights will be changed with γ and θ.

6. Conclusions

The presence of a FACTS device like UPFC on a double-circuit transmission line in a two-terminal system can substantially influence the apparent impedance seen by a distance relay. This phenomenon has been clearly demonstrated in this paper by varying the UPFC parameters, its location, fault resistance magnitude variations along with source impedance and other uncertainties for both line to ground and double line to ground faults. The ideal trip boundaries are derived clearly showing the influence of UPFC operating parameters. In real-time applications these boundaries need to be generated adaptively for issuing the necessary trip commands to the circuit breakers.

References

[1] L. Gyugyi, C.D. Schauder, S.L. Torgerson, A. Edris, The unified power flow controller: a new approach to power transmission control, IEEE Trans. Power Deliv. 10 (2) (1995) 1088–1097.
[2] L. Gyugyi, Unified power flow control concept for flexible AC transmission systems, IEE Proc. Gener. Transm. Distrib. 139 (4) (1992) 323–332.
[3] K.R. Padiyar, A.M. Kulkarni, Control design and simulation of unified power flow controller, IEEE Trans. Power Deliv. 13 (4) (1998) 1348–1354.
[4] IEEE/CIGRE, FACTS overview, Special Issue, 95tp108, IEEE Service Centre, NJ (1995).
[5] A.A. Girgis, A.A. Sallam, A.K. El-Din, An adaptive protection scheme for advanced series compensated (ASC) transmission lines, IEEE Trans. Power Deliv. 13 (1) (1998) 414–420.
[6] A.K. Jampala, S.S. Venkata, M.J. Damborg, Adaptive transmission protection: concepts and computational issues, IEEE Trans. Power Deliv. 4 (1) (1989) 177–185.
[7] Z. Zhizha, C. Deshu, An adaptive approach in digital distance protection, IEEE Trans. Power Deliv. 6 (1) (1991) 135–142.
[8] Y.Q. Xia, K.K. Li, A.K. David, Adaptive relay setting for stand-alone digital distance protection, IEEE Trans. Power Deliv. 9 (1) (1993) 480–491.
[9] Y.Q. Xia, A.K. David, K.K. Li, High resistance faults on multi-terminal lines: analysis, simulated studies an adaptive distance relaying scheme, IEEE Trans. Power Deliv. 9 (1) (1993) 492–501.
[10] P.J. Moore, R.K. Aggarwal, H. Jiang, A.T. Johns, New approach to distance protection for resistive double-phase to earth faults using adaptive techniques, IEE Proc. Gener. Transm. Distrib. 141 (4) (1994) 369–376.
[11] D.L. Waikar, S. Elangovan, A.C. Liew, Further enhancements in the symmetrical components based improved fault impedance estimation method. Part-I: Mathematical modeling, Elec. Power Syst. Res. 40 (1997) 189–194.
[12] D.L. Waikar, A.C. Liew, S. Elangovan, Further enhancements in the symmetrical components based improved fault impedance estimation method. Part-II: Performance evaluation, Elec. Power Syst. Res. 40 (1997) 195–201.
[13] Y. Liao, S. Elangovan, Digital distance relaying algorithm for first-zone protection for parallel transmission lines, IEE Proc. Gener. Transm. Distrib. 145 (5) (1998) 531–536.